

RSC Advances



This is an *Accepted Manuscript*, which has been through the Royal Society of Chemistry peer review process and has been accepted for publication.

Accepted Manuscripts are published online shortly after acceptance, before technical editing, formatting and proof reading. Using this free service, authors can make their results available to the community, in citable form, before we publish the edited article. This *Accepted Manuscript* will be replaced by the edited, formatted and paginated article as soon as this is available.

You can find more information about *Accepted Manuscripts* in the [Information for Authors](#).

Please note that technical editing may introduce minor changes to the text and/or graphics, which may alter content. The journal's standard [Terms & Conditions](#) and the [Ethical guidelines](#) still apply. In no event shall the Royal Society of Chemistry be held responsible for any errors or omissions in this *Accepted Manuscript* or any consequences arising from the use of any information it contains.

Air-expansion induced hierarchically porous carbonaceous aerogels from biomass materials with superior lithium storage properties

Pei Han^{a,1}, Bo Yang^{a,1}, Zhaozheng Qiu^a, Yajie You^a, Jing Jiang^a, Jianhong Liu^a, Jian Xu^b, Haosen Fan^{a,b*}, Caizhen Zhu^{a*}

^a*College of Chemistry and Chemical Engineering of Shenzhen University, Shenzhen 518060, China*

^b*Institute of Chemistry, Chinese Academy of Sciences, Beijing 100190, China*

Abstract

Traditional methods for the preparation of carbon aerogels, such as sol-gel method, hydrothermal method, freeze-drying method and direct carbonization of biomass materials, have been more and more limited for applications due to their high cost, complex process and the accompanying volume shrinkage in the preparation process. In this paper, we developed a novel air-expansion method for the preparation of porous carbonaceous aerogels with hierarchically macroporous, mesoporous and microporous structures from rice. The main advantage of air-expansion method is large-scale preparation, low cost, simple technique and most important keeping the initial shape/structure and avoiding the shrinkage of carbon aerogels owing to air-expansion process of rice generating many macroporous structures for supporting aerogel framework. When used as an anode for lithium ion batteries, rice-based carbonaceous aerogel exhibits a superior specific capacity and possesses a good rate capability. This study gives a better insight for the preparation of carbonaceous aerogel from other grains as well as its potential applications in lithium ion batteries.

Keywords: Puffed rice; Carbonaceous aerogel; biomass material; lithium ion batteries; anode

* Corresponding author. Tel/Fax: 86-755-26535427
E-mail address: czzhu@szu.edu.cn (C. Zhu), fhs@iccas.ac.cn (H. Fan)
¹ These authors contributed equally.

1. Introduction

In order to solve the increasing environmental issues and the finite fossil-fuel supplies, it is very important and urgent to develop alternative energy conversion and storage resources. Lithium ion batteries have been the main power source of the portable electronic devices in recent years due to its high energy density.[1,2] It's well known that graphite have been currently the most commonly used anode carbon material due to its low and flat potential plateaus, high coulombic efficiency and low cost. However, its limited theoretical capacity (up to 372 mAh g⁻¹) cannot completely satisfy with the requirements of the new applications such as electric and hybrid electric vehicles. Other anode materials such as metal oxides and silicon have high theoretical capacities, but the high price, environmental pollution and bad longterm cycling characteristics limits their further application.[3,4]

In the last ten years, graphene has been considered as the ideal candidates for the next generation anode materials owing to its excellent mechanical and electrical properties.[5-7] As a two-dimensional all-sp²-hybridized carbon material, graphene carbon atoms arrange in a honeycomb lattice with high accessible surface area (2630 m² g⁻¹).[8] However, the most commonly used method for preparation graphene by chemical oxidation has some drawbacks, such as complex and boring synthetic process, producing of environmentally hazardous wastes, as well as very low yield, which result in a high price of graphene and limit it pratical application.[9-11] Futhermore, most reports show that the actual electrochemical performances of graphene and graphene-based anode materials are much lower than the theoretical value because of the facile aggregation and restacking of graphene sheets by Vander Waals interactions among individual graphene sheets.[12,13] Hence, the exploitation of lowcost and effective carbon anode materials with high-rate and good cycling stability is the urgent and key requirements for lithium-ion battery technology. Recently, biomass with nature micro-nano holes derived porous carbon and carbon

aerogels have attracted much attention for the electrode materials of supercapacitor and lithium ion batteries because of their low cost, reproducibility, environmental friendliness and large specific surface area.[14-17] Therefore much effort has been made to synthesis the porous carbon materials obtained from all kind of biomass materials. For example, wu *et al.* have prepared low-cost and sponge-like carbonaceous flexible hydrogels and aerogels from crude biomass watermelon as the carbon source.[18] The final magnetite carbon aerogels exhibit an excellent capacitance properties and outstanding cycling stability after 1000 cycles of charge/discharge process. Tang *et al.* developed a new method to synthesize graphene from eggshell as high-performance electrode material for energy storage by a simple magnesiothermic reduction reaction.[19] Besides, other biomass materials such as rice husks,[20] peanut shells,[21] banana peels,[22] pomelo peels,[23] coconut shells,[24] starch[3] have been successfully used as carbon sources for preparing all kind of porous carbon materials as new type electrode materials for capacitor, lithium and sodium ion batteries.

In this paper, we demonstrate a novel air-expansion method for the preparation of hierarchically macro-, meso- and micro-porous carbonaceous aerogels used rice as the carbon source. Puffed rice is to rice as popcorn is to corn. During the puffing process, A porous spongy texture can be formed by the reaction of both starch and moisture when heated with the shell of grain. The typical method of puffing rice is “gun puffing”, where the rice is conditioned to the suitable moisture and pressurised to around 200 pressure per square inch (PSI). When the pressure is suddenly released, the pressure stored inside the kernel causes it to puff out. This method produces a puffed rice which is spongy in texture. After high temperature carbonization process, a novel carbonaceous aerogel with hierarchically macroporous, mesoporous and microporous structures was obtained. The air-expansion method used here thoroughly solved the high cost, complex gelatinization, drying process and shrinkage problem of carbon aerogels by the traditional method, such as sol-gel

method,[25] graphene based aerogels by hydrothermal method or freeze-drying method,[26] and single-step carbonization of biomass materials method.[27] Most important, the air-expansion method generates porous structure from natural non-porous biomass materials and exploits the scope of selecting biomass materials for the preparation of carbonaceous aerogels. The obtained porous carbonaceous aerogel here exhibits excellent electrochemical performance used as the anode materials of lithium ion batteries due to its extraordinary porous architecture and N-doped structure. This method not only open a new way to prepare carbonaceous aerogel from grain, but also find a potential application in anode materials for lithium ion batteries.

2. Experimental

2.1 Preparation of hierarchically porous carbonaceous aerogels

The puffed rice used in this research was prepared by “gun puffing”, where the rice was sealed into a pressure-tight metallic container and conditioned to the suitable moisture and pressurised to around 200 pressure per square inch (PSI). When the pressure was suddenly released, the pressure stored inside the kernel caused it to puff out. This method produced a puffed rice which is spongy in texture. Then the sample was carried into an argon-flowing tubular furnace for the pyrolysis process at different temperature of 500, 600 and 700°C for 1h with a heating rate of 5 °C/min. The obtained carbon was then ground into powders and refluxed with 2M HCl solution at 120 °C for 1h to remove the remaining impurities. The prepared product was thoroughly rinsed with DI water to ensure it was neutral and then dried 80°C over night in a vacuum oven. The obtained carbonaceous aerogels at 500, 600 and 700°C were named as PFC-500, PFC-600 and PFC-700, respectively.

2.2 Characterization

Morphology of all samples was characterized by scanning electron microscope (SEM, JEOL 7500F) and transmission electron microscope (TEM, JEOL JEM-2100F), respectively. X-ray

photoelectron spectroscopy (XPS) analysis was carried out on an ESCALab220i-XL electron spectrometer from VG Scientific. Al-K α radiation was used as the X-ray source and operated at 300W. Thermogravimetric Analysis (TGA) was tested using a STA409PC (NETZSCH) from 50 to 800 °C at air condition. N₂(at 77.3K) and CO₂(at 273K) sorption measurements were performed using 5 QUADRASORB SI/MP and Autosorb-1MP from Quantachrome Instruments, respectively. Samples were outgassed at 200°C under vacuum for 24h before measurements. Brunauer-Emmett-Teller (BET) and nonlinear density functional theory (NLDFT) methods were used for the surface area and pore size distributions (PSDs) using N₂ adsorption data, and Grand canonical Monte Carlo(GCMC) method was used for CO₂ adsorption data analysis. The crystalline structure was characterized by X-ray diffraction 10 (XRD) on a Micscience M-18XHF (with CuK α radiation) instrument. Raman spectra were taken by confocal HR800 spectrometer of HORIBA Jobin Yvon.

2.3 Electrochemical measurements

Carbon electrodes for electrochemical lithium insertion were prepared by blade-coating a slurry of 80% of PFC, 10% of sodium alginate (SA) and 10% super P dispersed in defined amount of DI 15 water on copper foil, followed by drying at 70°C for 6h and punched into circular discs for coin-cell fabrication. The electrolyte was 1M LiPF₆ dissolved in a mixture of ethylene carbonate (EC), dimethyl carbonate (DMC) and ethyl methyl carbonate (EMC) (in a volume ratio of 1:1:1). To test the electrochemical properties, 2032 type coin cells were assembled in an argon-filled glove box using lithium metal for the counter electrodes. The cells were electrochemically cycled 20 between 0.01V and 3V (at 0.1C under a constant current mode for both charge and discharge in the first cycle and cycled at different current rates thereafter using a cycle tester). The galvanostatic charge-discharge test was conducted by a Wu-Han land CT2001A testing system. Electrochemical impedance spectra (EIS) characterization were measured using a Solatron 1260 Impedance Analyzer.

3. Results and Discussion

As exhibited in Fig. 1a, a puffed and carbonized strategy is designed to prepare the hierarchically porous structure carbonaceous aerogel from rice. Firstly, rice became swell to form popcorn through puffing treatment, which develop many macroporous structure as the skeleton of carbonaceous aerogel. After carbonizing at argon atmosphere, lightweight carbonaceous aerogels were obtained with only about ten percents weight of popcorn but maintained their original shape and larger volume containing plenty of microporous and mesoporous structure. The carbonaceous aerogel by this air-expansion method greatly reduced the shrinkage of aerogel in comparasion to the method of direct carbonization of biomass materials. Since rice is the main grain in the world with great yield, it is open a new way to prepare carbonaceous aerogel with hierarchical porosity structure for potential application in energy storage.

The SEM iamges of the puffed rice and carbonized aerogels are presented in Fig. 2. It can be seen that through puffing treatment the rice shows a laminated structure with a smooth surface. However, Fig. 2b-d show the typical image of the puffed rice powders carbonized at different temperature. Many pores of different diameters, which can remarkably enhance the active surface area for lithium ion storage. For relatively low temperature (500 °C, Fig. 2b), the carbonaceous products roughly retain multilayer structure and as a result of the pyrolysis a number of macropores of different sizes formed on the carbon layer surface which is favorable for the intercalation of lithium ion. In contrast, the random layers before are destroyed and melt together more or less but more visible pores are found in the samples carbonized at 600°C and 700°C. The transmission electron microscopy (TEM) and HRTEM images in Fig. 1e reveals that there are many macropores, mesopores and a large amount of micropores within the PFC-600. Among them, the walls of the macropores and large mesopores consist of an amorphous texture and micropores (Fig. 1f), forming an interconnected structure. In the hierarchically porous structure, the mesopores

of the carbonaceous aerogel can provide a short ion-transport pathway, with a minimized inner-pore resistance. Interconnected micro-, meso-, and macropores can provide low-resistant ion channels to facilitate ion transportation, which can effectively improve the capacity of carbonaceous aerogel anode.

Fig. 3a shows the XRD patterns of the carbonaceous aerogels. The typical peaks of three samples centered at 25° and 43° can be assigned to (002) and (101) reflections of planes of hexagonal graphite, respectively.[28] Moreover, no sharp peaks in the XRD patterns of the three carbon areogels indicate they are in their amorphous state. which is beneficial for Li^+ intercalation and deintercalation.[29] Raman spectra in Fig. 3b demonstrate that the three samples show obvious the G band ($\sim 1595 \text{ cm}^{-1}$) and D band ($\sim 1380 \text{ cm}^{-1}$) which ascribe to the vibration of sp^2 -bonded carbon atoms in a 2D hexagonal lattice and disordered carbon or defective graphitic structures, respectively. The I_D/I_G intensity ratio is a measure of the disorder degree of obtained carbon areogels. The I_D/I_G ratio of the PFC-500 (0.79) is lower than that of the HPC-600 (0.78) and HPC-700 (0.87), suggesting a higher degree of defects and lower degree of graphitization at high carbonated temperature.

Fig. 4 show X-ray photoelectron spectroscopies (XPS) of the three carbonized samples, which were used to investigate the nature of the doped nitrogen species on the surface of carbonaceous aerogel. The different status of N has been well-documented for the existence into the carbon matrix. The high-resolution N1s core level XPS spectra of all samples can be fitted to three different 3 peaks, at 398.6, 400.1 and 400.9 eV, representing pyridinic N (N-6), pyrrolic or pyridonic N (N-5) and quaternary N (N-Q), respectively. It has been reported that N-5 and N-6 functional groups in the N-doped porous carbons are the most important functional groups for the improvement of energy storage performance. PFC-600 contains more pyridinic N compared to those of the samples PFC-500 and PFC-700 (Table S1), which is more favorable than pyrrolic-N

for lithium ions storage the increase of reversible capacity.

The effect of carbonization on the specific surface area and microstructure of carbonaceous aerogels are further studied by both $N_2(77.3K)$ as well as $CO_2(273K)$ sorption. As is shown in Fig. 5c, all N_2 adsorption isotherms of PFC samples did not close upon desorption in the measured pressure range, thus presenting extensive pressure hysteresis. It is probably owing to N_2 sorption at 77.3K can analysis a broad size range of micro- and meso-pores. However, in the case of our materials, there may be more ultramicropores($< 0.8nm$), hence N_2 sorption was affected by kinetic restrictions and could not provide a exact surface area data[30]. But even so, we can still obtain some mesopores information from PSDs(Fig. 5d) caculated from N_2 isotherms which presented mesopore size distributes in a range about 10nm. On the contrast, CO_2 sorption isotherms at 273K in Fig. 5a show good adsorption kinetics without hysteresis as compare to N_2 adsorption, due to the smaller kinetic diameter of CO_2 ($D(CO_2)=0.33nm$, $D(N_2)=0.36nm$) and higher thermal energy at a higher measurment temperature of 273K[31]. It can be seen that all CO_2 adsorption isotherms acquired at 273K show a leap in gas uptake, correlated with the elimination of volatile species. PFC-700 shows a continuous increase of adsorption capacity in the whole pressure range than that of PFC-500 and PFC-600, and surface areas increase with the rise of carbonized temperature since more volatile species formate in higher temperature for PFC-500 ($384.31 m^2 g^{-1}$), PFC-600 ($389.19 m^2 g^{-1}$) and PFC-700 ($461.61 m^2 g^{-1}$), respectively. Pore size distributions (PSDs, Fig. 5b) showed a ultramicropores range of 0.3 to 0.7 nm. From the SEM images and PSDs, as a result, the porous carbonaceous aerogels possess a hierarchically macro-, meso- and microporous structures.

The electrochemical performance of carbonaceous aerogel PFC-600 as anode materials for lithium ion batteries was characterized by cyclic voltammograms (CV) and charge-discharge curves. The CV curve recorded in the first three cycles of the PFC-600 (Fig. 6a) are typical profiles for carbonaceous anode materials with the shape matching well with the charge-discharge

profiles.²⁸ Fig. 5b-d show the representative charge-discharge curves of the PFC-500, PFC-600 and PFC-700 at a current density of 37mAh g^{-1} , respectively. In the first cycle, the charge-discharge curves of the PFC-600 exhibit an high first-cycle discharge and charge capacities of 1180 and 750 mAh g^{-1} and a Coulombic efficiency of 63.6%. higher than that of the PFC-500 and PFC-700 (1340/680 mAh g^{-1} and 745/482 mAh g^{-1} , respectively) (Fig. 6b and c). The initial Coulombic efficiency of the three electrodes is not high because of the large irreversible capacity during the first cycle such as the decomposition of electrolyte, some irreversible processes such as the formation of a solid-electrolyte interface layer on the surface of electrodes[32]. In the second cycle, PFC-600 electrode shows a discharge capacity of 696 mAh g^{-1} following by a charge capacity of 648 mAh g^{-1} , accompanying a increased Coulombic efficiency of about 93.1%. After 30 cycles, the reversible capacity of the PFC-600 is maintained at 458 mAh g^{-1} with a stabilized Coulombic efficiency around 98.4%, while the other two samples show apparently dropped capacities to 373 mAh g^{-1} and 342 mAh g^{-1} , respectively.

Fig. 7a shows the cycling performance of the PFC-500, PFC-600, PFC-700. Obviously, the PFC-600 shows a better cycling stability than PFC-500 and PFC-700 at a constant current density of 0.1 C. It can be seen PFC-600 still keep 505 mAh g^{-1} after 110 cycles while the reversible capacity of PFC-700 and PFC-500 fades rapidly to lower than 400 mAh g^{-1} . In other reported researches that use biomass materials as carbon source, maybe their materials can show a higher specific capacity than ours [20-24], but almost of them use KOH or the other chemical agents as pore-agents, and if they carbonized their materials directly without KOH, a relative lower specific capacity about only 200 mAh g^{-1} will be obtained. Consequently, our environmental-friendly air-expansion method can indeed induce pores into materials and improve their electrochemical properties without the usage of any chemical reagent.

For the reasons of improved specific capacity through air-expansion method, firstly and crucial

one is the induced porous structure as presented in SEM images and N_2 / CO_2 adsorption isotherms, which is beneficial for Li^+ storage. The other one reason is heteroatom dopants such as H atom and N atom, since Li atoms can bind in the vicinity of the H atoms in the hydrogen-containing carbons and have a stronger interaction with N atom because of the hybridization of nitrogen lone pair electrons with the π electrons. There is an optimum carbonized temperature since high temperature can develop more pores in structure and high surface area, but meanwhile, more advantageous heteroatoms like H atom and N atom will lose with temperature rising (Table. S1). It is believed to be related to a trade off between increasing surface area and the loss of useful heteroatoms. As a result, PFC-600 balanced the two factors, and showed the best electrochemical properties.

Fig. 7b shows the rate capabilities of three samples at various current densities from 0.1C to 10C, each for 10 cycles. It is clearly that all examples show excellent cyclic capacity retention at each current density. Especially for PFC-600, when the charge-discharge current density increase from 0.1 C to 10 C and then turns back to 0.1 C, the reversible capacities are still as high as 534 mAh g^{-1} . The carbonaceous aerogels presents good cyclic and rate performance mainly attributed to its hierarchically macroporous, mesoporous and microporous structures, which can provide a good channel for Li^+ intercalation and deintercalation.

The Nyquist diagrams in Fig. 8 show the impedance variation of three carbonaceous aerogel examples. All the three electrodes show similar plots consisting of a depressed semicircle in the high-medium frequency regions and a straight line in the low-frequency region, corresponding to the SEI film resistance (or contact resistance) and the charge transfer resistance on the interface of the electrode and the electrolyte (R_{SEI}) and the semi-infinite diffusion of the lithium ions in the carbonaceous aerogels electrodes (R_e), respectively.[33-35] The value of R_{SEI} is the diameter of the semicircle in real part, which is the sum resistance of the electrochemical cell system and one of the limiting factors for the power density of electrodes. It is obvious that the diameter of the

semicircle of the PFC-700 is smaller than that of PFC-500 and PFC-600 electrodes, implying that it possesses the highest electrical conductivity and the more easily charge transfer reaction for lithium ion insertion and extraction of all the three samples. The equivalent circuit has been set up as shown in the inset of Fig. 8.

5 4. Conclusions

In summary, a facile and economic air-expansion method was employed to prepare hierarchically porous nitrogen-rich carbonaceous aerogel using rice as a carbon source. The obtained porous carbonaceous aerogel maintain the pristine structure of popcorn and display large specific surface area due to its hierarchically macroporous, mesoporous and microporous structure, which exhibits
10 high specific capacity and ultra-high rate capability. This approach could become an effective way for the preparation of carbonaceous aerogel from other grain, such as corn, soybean and wheat by the air-expansion method, also making such porous carbonaceous aerogel promising anode materials for the application in the lithium ion batteries or supercapacitors.

Acknowledgements

15 This work was supported by the National Natural Science Foundation of China (NSFC) (Grant No. 21304059), National High-tech R&D Program (863) (2015AA03A204), the Guangdong Doctor Startup fund(S2013040015706), Shenzhen Science and Technology Research Grant (JCYJ20140418091413553).

20 REFERENCES

[1] M. Winter, R. J. Brodd, What are batteries, fuel cells, and supercapacitors, Chem Rev. 104 (2004) 4245-70.

- [2] Nitta N, Yushin G, High-Capacity Anode Materials for Lithium- Ion Batteries: Choice of Elements and Structures for Active Particles, Part Part Syst Charact. 31 (2014) 317-36.
- [3] Xiao C, Du N, Shi X, Zhang H, Yang D, Large-scale synthesis of Si@C three-dimensional porous structures as high-performance anode materials for lithium-ion batteries, J Mater Chem A. 2 (2014) 20494-9.
- [4] Huang Y, Chen C, An C, Xu C, Xu Y, Wang Y, Synthesis of Cobalt based Complexes and conversion to Co_3O_4 nanoparticles as a high performance anode for lithium ion battery, Electrochim. Acta 145 (2014) 34-9.
- [5] Wang R, Xu C, Sun J, Gao L, Three-Dimensional Fe_2O_3 Nanocubes/Nitrogen-doped Graphene Aerogels: Nucleation Mechanism and Lithium Storage Properties, Sci Rep 4 (2014) 7171-7.
- [6] Liu X, Gao Y, Jin R, Luo H, Peng P, Liu Y, Scalable synthesis of Si nanostructures by low-temperature magnesiothermic reduction of silica for application in lithium ion batteries, Nano Energy 4 (2014) 31-8.
- [7] Kucinskis G, Bajars G, Kleperis J, Graphene in lithium ion battery cathode materials: A review, J Power Sources 240 (2013) 66-79.
- [8] Srivastava M, Singh J, Kuila T, Layek R, Kim N, Lee J, Recent advances in graphene and its metal-oxide hybrid nanostructures for lithium-ion batteries, Nanoscale 7 (2015) 4820-68.
- [9] Zai J, Qian X, Three dimensional metal oxides-graphene composites and their applications in lithium ion batteries, Rsc Adv 5 (2015) 8814-34.
- [10] Huang L, Wu B, Yu G, Liu Y, Graphene: learning from carbon nanotubes. J Mater Chem 21 (2011) 919-29.
- [11] Kovtyukhova N, Ollivier P, Martin B, Mallouk T, Chizhik S, Buzaneva E, Layer-by-Layer Assembly of Ultrathin Composite Films from Micron-Sized Graphite Oxide Sheets and Polycations, Chem Mater 11 (1999) 771-8.

- [12] Botas C, Alvarez P, Blanco P, Granda M, Blanco C, Santamaria R, Graphene materials with different structures prepared from the same graphite by the Hummers and Brodie methods. *Carbon* 65(2013) 156-64.
- [13] Fan H, Wang H, Zhao N, Xu J, Pan F, Nano-porous architecture of N-doped carbon nanorods grown on graphene to enable synergetic effects of supercapacitance, *Sci Rep* 4 (2014) 7426-7.
- [14] Zhang L, Zhou R, Zhao X, Graphene-based materials as supercapacitor electrodes, *J Mater Chem* 20 (2010) 5983-92.
- [15] Fan H, Zhao N, Wang H, Xu J, Pan F, 3D conductive network-based free-standing PANI-RGO-MWNTs hybrid film for high-performance flexible supercapacitor, *J Mater Chem A* 2 (2014) 12340-7.
- [16] He X, Ling P, Qiu J, Yu M, Zhang X, Yu C, Efficient preparation of biomass-based mesoporous carbons for supercapacitors with both high energy density and high power density. *J Power Sources* 240 (2013) 109-13.
- [17] Ruan C, Ai K, Lu L, Biomass-derived carbon materials for high-performance supercapacitor electrodes, *Rsc Adv* 4 (2014) 30887-95.
- [18] Park M, Ryu J, Kim Y, Cho J, Corn protein-derived nitrogen-doped carbon materials with oxygen-rich functional groups: a highly efficient electrocatalyst for all-vanadium redox flow batteries, *Energy Environ. Sci.* 7(2014) 3727-35.
- [19] Liang H, Wu Z, Chen L, Li C, Yu S, Bacterial cellulose derived nitrogen-doped carbon nanofiber aerogel: An efficient metal-free oxygen reduction electrocatalyst for zinc-air battery, *Nano Energy* 11 (2015) 366-76.
- [20] Wu X, Wen T, Guo H, Yang S, Wang X, Xu A, Biomass-Derived Sponge-like Carbonaceous Hydrogels and Aerogels for Supercapacitors, *Acs Nano* 7 (2013) 3589-97.

- [21] Tang H, Gao P, Liu X, Zhu H, Bao Z, Bio-derived calcite as a sustainable source for graphene as high-performance electrode material for energy storage, *J Mater Chem A* 2 (2014) 15734-9.
- [22] Wang L, Schnepf Z, Titirici M, Rice husk-derived carbon anodes for lithium ion batteries, *J Mater Chem A* 1 (2013) 5269-73.
- 5 [23] Ding J, Wang H, Li Z, Cui K, Karpuzov D, Tan X, Peanut shell hybrid sodium ion capacitor with extreme energy-power rivals lithium ion capacitors, *Energy Environ. Sci.* 8 (2015) 941-55.
- [24] Lotfabad EM, Ding J, Cui K, Kohandehghan A, Kalisvaart WP, Hazelton M, High-Density Sodium and Lithium Ion Battery Anodes from Banana Peels, *ACS Nano* 8 (2014) 7115-29.
- [25] Hong K, Qie L, Zeng R, Yi Z, Zhang W, Wang D, Biomass derived hard carbon used as a high
10 performance anode material for sodium ion batteries, *J Mater Chem A* 2(2014) 12733-8.
- [26] Jain A, Aravindan V, Jayaraman S, Kumar PS, Balasubramanian R, Ramakrishna S, Activated carbons derived from coconut shells as high energy density cathode material for Li-ion capacitors, *Sci Rep* 3 (2013) 3002-6.
- [27] Li C, Shi G, Three-dimensional graphene architectures. *Nanoscale* 4 (2012) 5549-63.
- 15 [28] Li Y, Samad YA, Polychronopoulou K, Alhassan SM, Liao K, From biomass to high performance solar-thermal and electric-thermal energy conversion and storage materials, *J Mater Chem A* 2 (2014) 7759-65.
- [29] Qie L, Chen W, Wang Z, Shao Q, Li X, Yuan L, Nitrogen-Doped Porous Carbon Nanofiber Webs as Anodes for Lithium Ion Batteries with a Superhigh Capacity and Rate Capability, *Adv Mater* 24
20 (2012) 2047-50.
- [30] Jekaterina Heromenok, Hens Weber, Restricted Access: On the Nature of Adsorption/Desorption Hysteresis in Amorphous, Microporous Polymeric Materials. *Langmuir* 29(2013) 12982-12989.

- [31] Linghui Yu, Camillo Falco, Jens Weber, Robin H. White, Hane Y. Howe, Maria-Magdalena Titirici, Carbohydrate-Derived Hydrothermal Carbons: A Thorough Characterization Study. *Langmuir* 28(2012) 12373-12383.
- [32] Pan D, Wang S, Zhao B, Wu M, Zhang H, Wang Y, Li Storage Properties of Disordered Graphene
5 Nanosheets. *Chem Mater* 21 (2009) 3136-42.
- [33] Chen L, Zhang Y, Lin C, Yang W, Meng Y, Guo Y, Hierarchically porous nitrogen-rich carbon derived from wheat straw as an ultra-high-rate anode for lithium ion batteries, *J Mater Chem A* 2 (2014) 9684-90.
- [34] Song R, Song H, Zhou J, Chen X, Wu B, Yang H, Hierarchical porous carbon nanosheets and
10 their favorable high-rate performance in lithium ion batteries, *J Mater Chem* 22 (2012); 12369-74.
- [35] Fan H, Zhao N, Wang H, Long Y, Li X, Xu J, Noncovalent fabrication and electrochemical capacitance of uniform core-shell structured polyaniline-carbon nanotube nanocomposite, *RSC Adv* 2 (2012) 11887-91.

Figures



Fig. 1 - Schematic illustration of the air-expansion method for hierarchically porous carbon aerogel from rice.

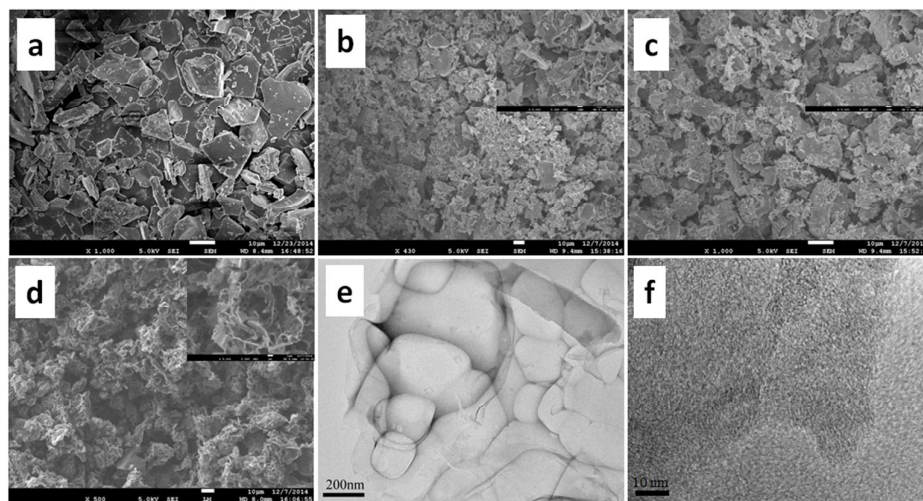


Fig. 2 - SEM images of (a) Original puffed rice, (b) PFC-500, (c) PFC-600, (d) PFC-700 and (e)(f) TEM images and high resolution images of PFC-600

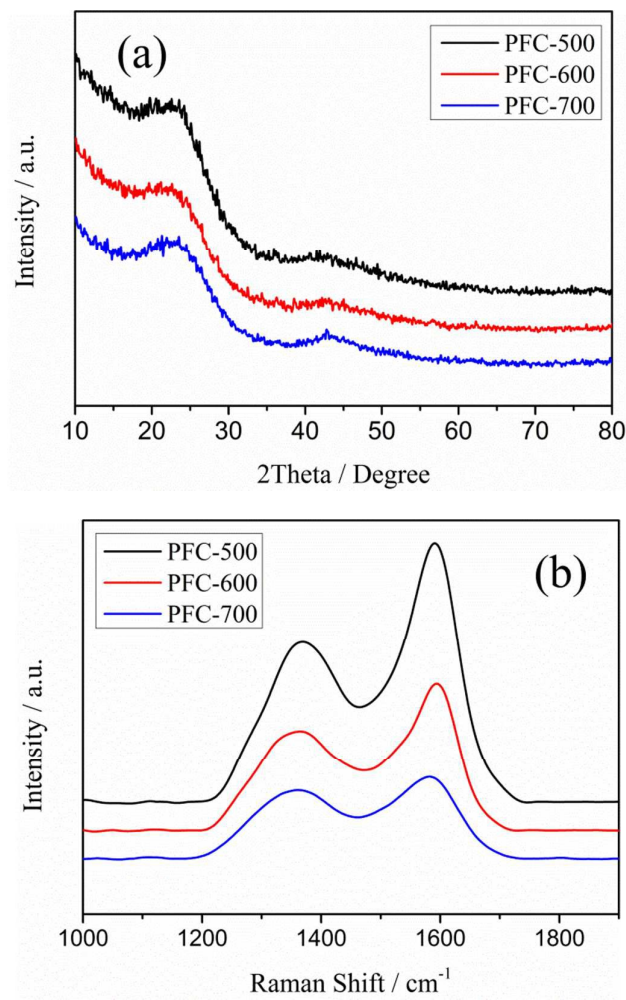


Fig. 3 - XRD and Raman spectra of PFC-500, PFC-600 and PFC-700.

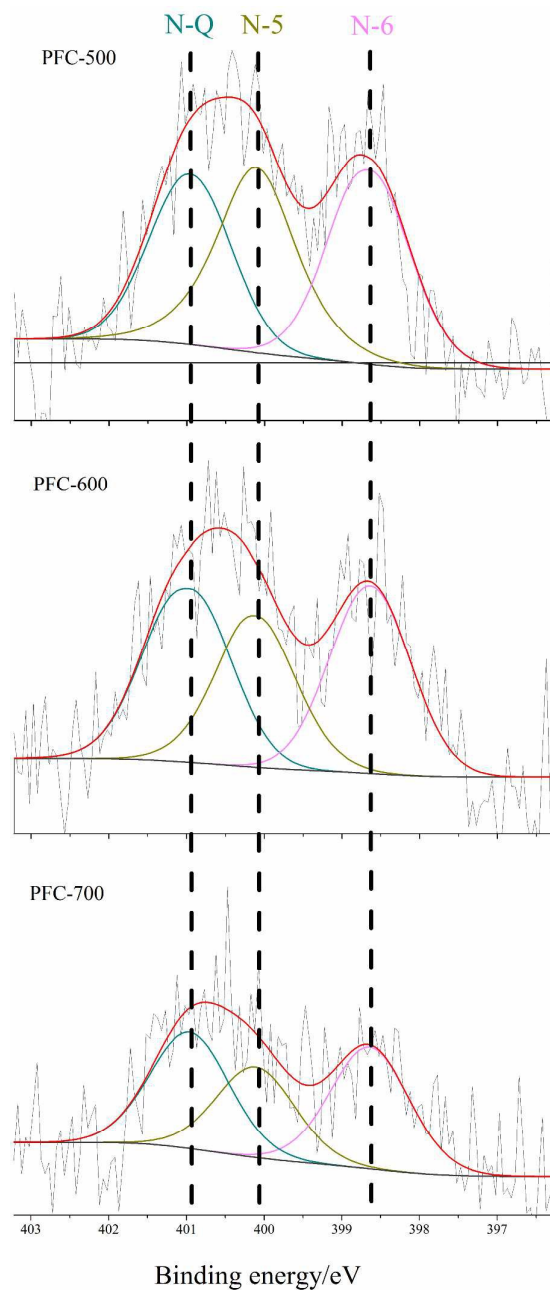
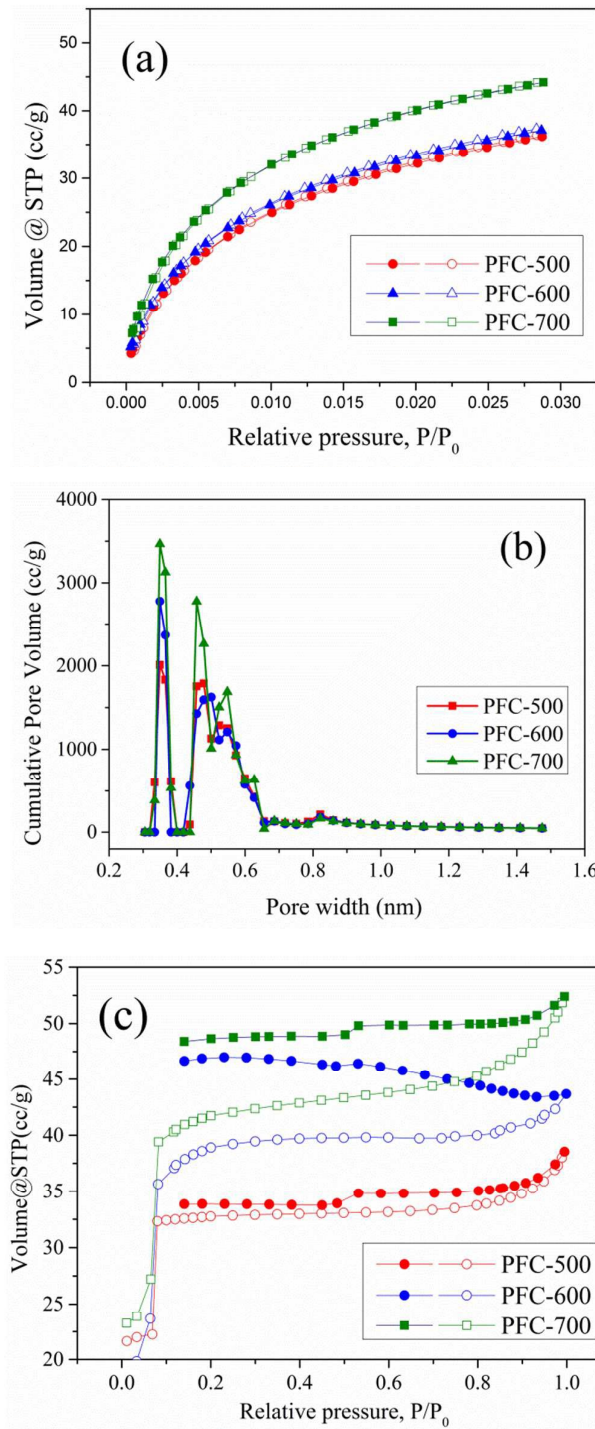


Fig. 4 - N1s XPS spectra for PFC-500, PFC-600 and PFC-700.



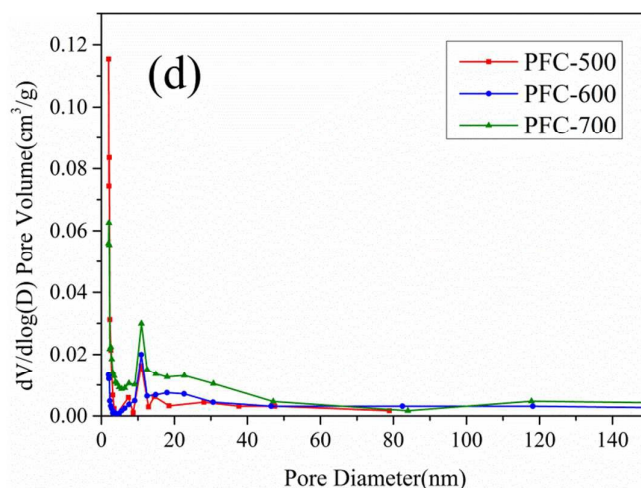


Fig. 5 –(a), (c) CO₂ and N₂ sorption isotherms and (b),(d) PSDs calculated from CO₂ and N₂ sorption isotherms, respectively.

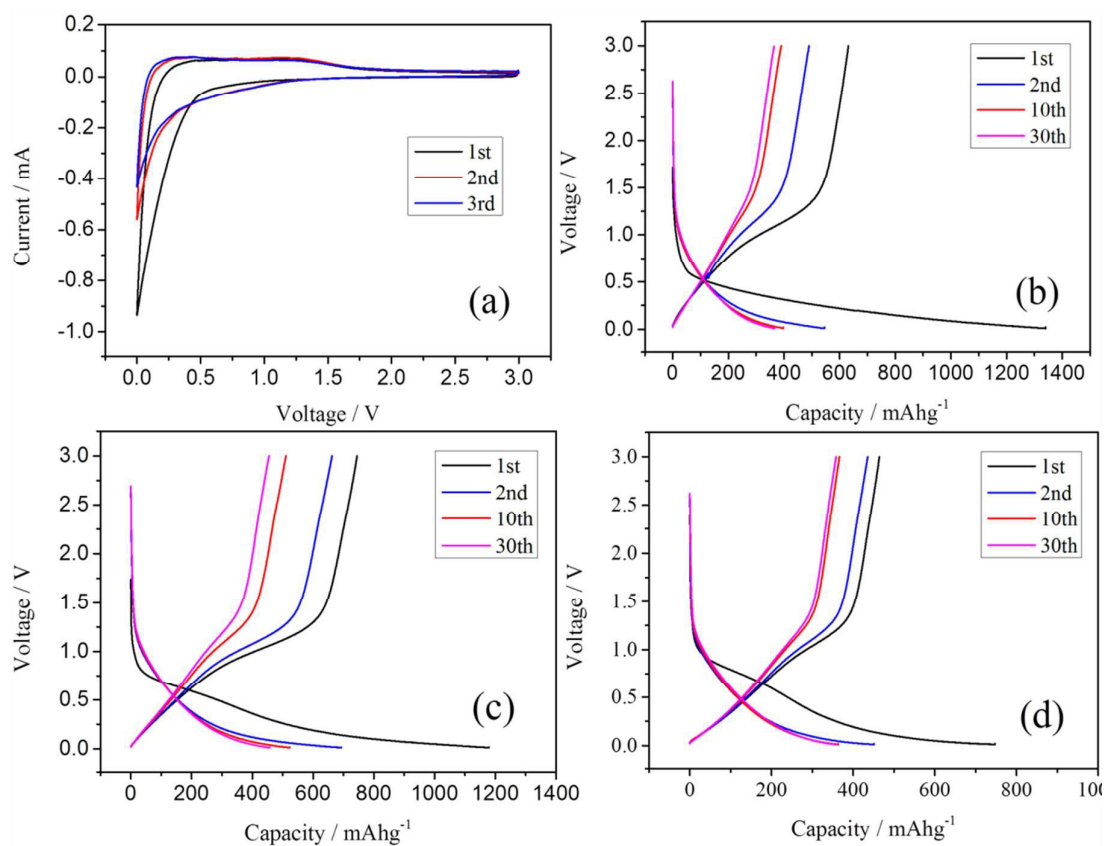


Fig. 6 - (a) Cyclic voltammograms of the PFC-700 at a scan rate of 0.1 mV s⁻¹; charge and discharge curves of (b) PFC-500, (c) PFC-600, (d) PFC-700 at 0.1C.

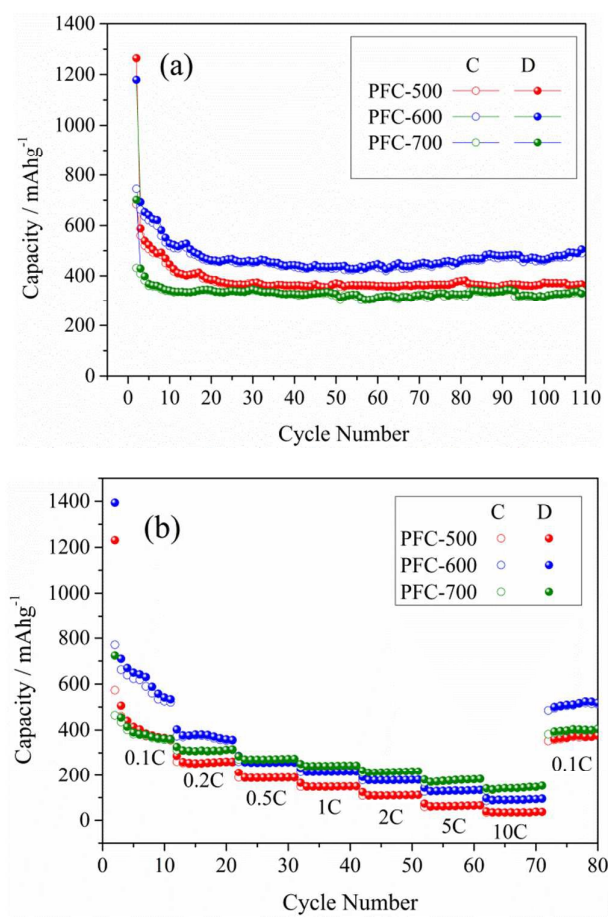


Fig. 7 - (a) Cycling performance of the PFC-500, PFC-600 and PFC-700; (b) the capacity performance of the PFC-500, PFC-600 and PFC-700 at different cycling rates.

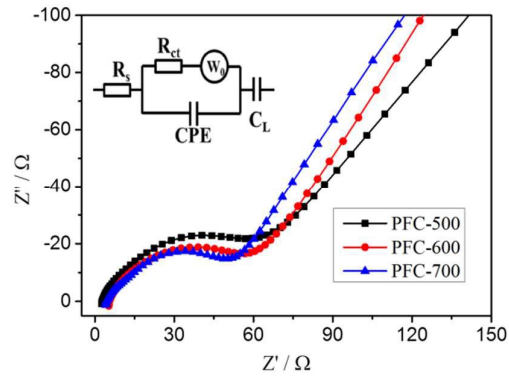


Fig. 8 - Typical Nyquist plots of PFC-500, PFC-600 and PFC-700.